Pergamon

Cement and Concrete Research 29 (1999) 1189–1200

CEMENT AND CONCRETE RESEARCH

The effect of metal contaminants on the formation and properties of waste-based geopolymers

J.G.S. van Jaarsveld, J.S.J. van Deventer*

Department of Chemical Engineering, The University of Melbourne, Parkville, Victoria 3052, Australia

Received 9 October 1998; accepted 18 January 1999

Abstract

The stabilisation and solidification of waste materials by the technology of geopolymerisation is receiving increasing attention from researchers; immobilisation of metal contaminants in these structures seems to be a viable alternative to present stabilisation techniques. This paper presents some experimental evidence concerning the effect of the inclusion of mainly Cu and Pb on the physical and chemical characteristics of geopolymers manufactured from fly ash. A variety of experimental and analytical techniques were used in this investigation, including compressive strength testing, specific surface area analyses, transmission electron microscopy, nuclear magnetic resonance, X-ray diffraction, and infrared spectroscopy. It was found that contaminants are being immobilised through a combination of chemical bonding and physical encapsulation. The nature of the contaminant seems to have a fairly large effect on both the physical and chemical characteristics of the final product, with subsequent long-term implications as far as durability is concerned. It is therefore concluded that a definite interaction exists between matrix-forming components and the immobilisation of the contaminant, where the amount of contaminant is a critical factor in the analysis.

Keywords: Amorphous material; Microstructure; Transmission electron microscopy; Fly ash; Lead

1. Introduction

Previous studies [1–4] have proposed the possible applications of geopolymers in the immobilisation of toxic metals, although few have presented substantial experimental data in order to quantify the relationship between heavy metal and geopolymer paste after structural integrity has been obtained. Describing this complex system is further complicated by the fact that many different waste materials can serve as reagents for geopolymerisation reactions with a whole range of heavy metals immobilised. This leads to numerous interactions between the contaminant and the host material, constituting the bulk of the geopolymer phase, that makes most observations fairly difficult to explain by conventional means. In this paper we have therefore resorted to a combination of analytical techniques in order to better quantify these interactions, although much still needs to be done before this aspect of geopolymerisation will be fully understood. In order to utilise waste-based geopolymers as permanent stabilisation and solidification systems in heavy metal containment, the base of knowledge regarding the leaching and long-term behaviour of contaminants immobilised in geopolymeric structures needs to be expanded and that is the ultimate aim of this paper.

2. Background and literature

It was mentioned previously [5] that among others the inclusion of a heavy metal in a geopolymer structure is thought to also change the nature of the compound in either a physical or chemical way. Previous authors [3] have acknowledged and speculated as to the nature of this heavy metal inclusion without any definite conclusions. Apart from the present study the only other available information regarding the immobilisation of heavy metals in geopolymers is part of a Canadian study completed in 1988 [6]. This investigation utilised a geopolymer binder (commercially available at that time) that was mixed with mine tailings from different sources and tested for metal immobilisation by regulatory environmental leaching procedures. The present investigation does not make use of the addition of a commercially available binder, but instead utilises the reactive properties of fly ash and kaolin to create the necessary geopolymeric binder. The behaviour of various metals under leaching conditions, however, can still be compared and

* Corresponding author. Tel.:+61-3-9344-6620; fax:+61-3-9344- 4153.
E-mail address: jsj.van_deventer@chemeng.unimelb.edu.au (J.S.J. van Deventer)

0008-8846/99/$ – see front matter
PII: S0008-8846(99)00032-0

Table 1
Composition of fly ash used as determined by fusion and XRF analysis (mass%)

Element as oxide	SASOL fly ash	Tarong fly ash
SiO_2	50.1	61.4
Al_2O_3	28.3	33.0
CaO	8.2	0.6
Fe_2O_3	4.0	1.1
MgO	2.0	0.3
TiO_2	1.5	2.0
Na_2O	0.5	0.1
K_2O	0.9	0.1
SO_3	0.4	0.0
Loss on ignition	4.1	1.4

evaluated since the mechanism of immobilisation is not thought to be significantly different in these two cases. The reason for this is the fact that in each case the chemical conditions of synthesis were quite similar. A study [7] concerning the immobilisation of intermediate-level radioactive waste with commercially produced geopolymer binders was completed in the early 1990s and leaching experiments conducted using both water and brine solutions.

For the purpose of this study various factors affect the eventual mechanical and chemical properties of the finished product. These include the immobilisation of the heavy metal, the thermal history of the reagents used, the type and amount of alkali metal cations present, as well as certain physical considerations such as particle size and ease of mixture of the various reagents. Only the first factor will be considered here, although it should be kept in mind that most of these factors are interdependent. It is evident that in each case where metals are being immobilised in an impermeable structure the nature of the metal ion either physically or chemically influences the structure forming around it, resulting in different immobilisation efficiencies for different metal ions. One important question that remains is whether the metal ion is physically or chemically bonded into the geopolymer structure during synthesis and also into which phases this bonding will preferably take place.

3. Methods

3.1. Materials

Fly ash used in the synthesis of matrices E1, E2, F1, F2, G1, and G2 was obtained from SASOL at Sasolburg, South Africa, and fly ash used in matrices H1 to H4 was obtained from the Tarong power station in Queensland, Australia. Both fly ashes are of coal origin, with d_{50}-values of around 12 micron and chemical compositions as shown in Table 1. Kaolinite, grade HR1, was obtained from Commercial Minerals, Sydney, Australia. In the preparation of matrices E1 and E2, metakaolinite was used; it was manufactured by calcining the above-mentioned kaoline at 600°C for 6 h as described by Madani [8]. All experiments were performed using the same batches of reagents and starting materials. Distilled water was used throughout.

3.2. Synthesis

Sample preparation was performed as described previously [2] with at least a 7-day waiting period before any tests were performed. In each case the samples were cast in 50-mm cubes, vibrated for 5 min, and allowed to set at 30°C for 24 h before being removed from the moulds and kept at room temperature for another 6 days. Heavy metal cations were added to the reaction mixture during mixing as solutions of their nitrate salts in water except in the case of arsenic where an oxide was used. Tables 2 and 3 summarise the compositions of the main matrices under discussion. It could well be noted that the amount of NaOH and KOH used in producing matrices E1, E2, F1, F2, G1, and G2 was chosen such as to provide for equal molar amounts of Na and K present in the structures of all the matrices in Table 2.

3.3. Compressive strength testing

Compressive strength testing was performed as per AS 1012.9 [9] using three 50-mm cubes of each sample and averaging the experimental values obtained. All samples were tested after 14 days. An Amsler FM 2750 (Roell Amsler, Gottmodingen, Germany) compressive strength-testing apparatus was used.

Table 2
Compositions of matrices prepared from SASOL fly ash (mass%)

Matrix	Contaminant	Alkali metal	Clay	Water/fly ash mass ratio	Al_2O_3/SiO_2 mass ratio
E1	Cu, 0.1	KOH, 5.0	Metakaolinite, 16.0	0.2	0.57
E2	Pb, 0.1	KOH, 5.0	Metakaolinite, 16.0	0.2	0.57
F1	Cu, 0.1	NaOH, 3.7	Kaolinite, 15.0	0.2	0.57
F2	Pb, 0.1	NaOH, 3.7	Kaolinite, 15.0	0.2	0.57
G1	Cu, 0.1	KOH, 5.0	Kaolinite, 15.0	0.2	0.57
G2	Pb, 0.1	KOH, 5.0	Kaolinite, 15.0	0.2	0.57

Table 3
Compositions of matrices prepared from Tarong fly ash (mass%)

Matrix	Contaminant	Alkali metal	Clay	Water/fly ash ratio	Al_2O_3/SiO_2 ratio
H1	Cu, 0.1	KOH, 5.0	Kaolinite, 14.0	0.43	0.57
H2	Pb, 0.1	KOH, 5.0	Kaolinite, 14.0	0.43	0.57
H3	Pb, 0.2	NaOH, 6.0	Kaolinite, 14.0	0.45	0.57
H4	Cu, 0.2	NaOH, 6.0	Kaolinite, 14.0	0.45	0.57

3.4. Specific surface area, infrared analysis, and X-ray diffraction

The Brunauer Emmet Teller (BET) surface areas were determined for all samples by using a Micromeritics Flowsorb ASAP 2020 (Micromeritics, Norcross, GA, USA) with a 30/70 ratio of N_2 and He and degassing for 18 h at 95°C. Infrared spectra were recorded on a Mattson Galaxy 2020 (Mattson Instruments, Madison, WI, USA) spectrometer using the KBr pellet technique (0.5 mg powder sample mixed with 250 mg of KBr). X-ray powder diffraction data were obtained for all samples using a Philips PW 1800 (Philips Equipment, Moorebank, NSW, Australia) diffractometer with CuKα radiation.

3.5. Nuclear magnetic resonance and transmission electron microscopy

Nuclear magnetic resonance (NMR) spectra were recorded using the Magic Angle Spinning (MAS) technique. ^{29}Si and ^{27}Al spectra were recorded at spinning speeds of 15 kHz (^{27}Al) and 4 kHz (^{29}Si) for matrices F1 and F2. Certain samples were also submitted to investigation by transmission electron microscopy (TEM) on a JEOL CS 100 TEM (Joel Asia, Singapore) fitted with an X-ray microanalysis system. The specimens were prepared by mechanically grinding the powder in ethanol, followed by ultrasonic agitation and precipitation on an amorphous carbon film. Electron diffraction data were obtained by manually measuring diffraction circle radii and calculating d-spacing values from the latter data, while taking into account the other microscope parameters.

3.6. Leaching tests

Samples submitted to leaching tests were crushed and sieved into particle-size fractions, the latter being leached until equilibrium conditions were obtained. Leaching of each particle-size fraction was conducted using a modified TCLP [2,10] procedure utilising acetic acid buffered at pH = 3.3 by analytical grade sodium acetate. The liquid/solid ratio was kept at 1:25 and the temperature controlled at 30°C. Equilibrium tests on matrices were conducted by the use of stirred vessels with overhead impellers. This technique allowed for equilibrium to be attained in around 24 h with sampling performed periodically over a 24-h period. Sampling was conducted by syringe and the total sampling volume never exceeded 10% of the fluid volume, thus creating an average error of 5%. In a separate set of experiments the matrices of Table 2 were also submitted to leaching by hydrochloric acid at pH = 3.3 with external pH control. Concentrations of all metals were determined using a Perkin Elmer Optima 3000 ICP-OES (Perkin Elmer, Norwalk, CT, USA), with scandium and/or cadmium as internal standard.

Table 4
Ionic radii of selected ions [11]

Ion	Radius (Å)
Cu^{2+}	0.72
Fe^{3+}	0.64
Cd^{2+}	0.97
As^{5+}	0.46
Pb^{2+}	1.20
Hg^{2+}	1.10

4. Results and discussion

4.1. General

It was noted previously [2,7] that two of the main factors that influence the incorporation of an ion into a geopolymer structure are thought to be the ionic size (Table 4) and valence of a specific ion [11]. Leaching data obtained by Davidovits et al. [3] show a reasonable correlation between ionic size and leaching efficiency when compared with published values of ionic sizes for the different ions (Table 5). It is also clear from the table that some exceptions could occur depending on the oxidation state of the ion at the time of leaching (this will greatly influence the ionic size).

Table 5
Comparison of immobilisation efficiencies (%) in geopolymerised base-metal mine tailings [3] with ionic radii of ions

Element	Immobilisation efficiency	Radius (Å) [11]
Cu	98	0.72/0.96
Cd	85	1.14/0.97
Pb	60	1.20
Mo	60	0.93
Cr	50	0.89/0.63
Zn	40	0.74
Ni	15	0.69
V	12	0.59

Table 6
Compressive strengths after 14 days (MPa)

Matrix	Contaminant	Alkali metal	Compressive strength
E1	Cu (0.1%)	K	28.1
E2	Pb (0.1%)	K	33.7
H1	Cu (0.1%)	K	4.5
H2	Pb (0.1%)	K	7.3
H2b	Pb (0.2%)	K	9.0
H3	Pb (0.2%)	Na	18.1
H4	Cu (0.2%)	Na	16.5

In this study, mainly Cu and Pb ions were used because of their similar valence numbers but different ionic radii. It should also be noted, however, that in highly heterogeneous systems such as those discussed by the CANMET report [6] as well as that of the present discussion it is expected that some competition exists between different metals regarding their incorporation possibilities into a geopolymeric structure. No study to date has optimised the loading of metal contaminants onto a geopolymer structure and in most cases the limiting factors are based on final strength, mixing, and other physical processing requirements.

4.2. Compressive strength

It is significant to note that the inclusion of Pb instead of Cu serves to strengthen the structure in terms of the final compressive strengths achieved (Table 6). This is true in the case of E1 and E2, H1 and H2, as well as H3 and H4. In each case the matrices contain equal mass amounts of the heavy metal although the molar amounts would differ and there would be fewer Pb ions present in each case than in the corresponding matrix containing Cu. Doubling of the mass amount of Pb ions in matrix H2b resulted in an even stronger product compared to H2 and it should be remembered that both H3 and H4 also have double the amount of metal ions if compared to H2 and H1, respectively, which results in quite substantial increases in compressive strength despite different alkali metal activators used. It is also evident from Table 7 that the specific surface area of the matrices that contain lead is higher than that of the corresponding Cu-containing matrices. This is not at all what would be expected from a structural point of view where the stronger sample could be expected to have less porosity. It therefore seems a reasonable assumption that although the Pb ion influences the structure in terms of causing increased porosity this effect is offset by its contribution to structural strength in another way, such as through its much larger ionic radius compared with that of Cu.

Table 7
BET surface areas for different matrices (m^2/g)

Matrix	Contaminant	Alkali metal	Specific surface area
E1	Cu (0.1%)	K	12.1
E2	Pb (0.1%)	K	16.7
H1	Cu (0.1%)	K	9.3
H2	Pb (0.1%)	K	12.2
H3	Pb (0.2%)	Na	7.8
H4	Cu (0.2%)	Na	4.3

Table 8
Compressive strength (MPa), porosity (%), and permeability (cm/s) data from CANMET report [6]

Matrix	Compressive strength	Porosity	Permeability
MW	3.3	23.5	1.2×10^{-4}
KK	2.7	29.2	1.1×10^{-5}
P	1.2	32.3	6.2×10^{-8}

Experimental data from the CANMET report is summarised in Table 8 and show that the expected relationship between compressive strength and porosity does exist, although permeability measurements again contradict these findings, with the most porous matrices being the least permeable and the strongest (least porous) matrices being the most permeable. Although this apparent contradiction could be a result of the measuring techniques used, it also seems to be an indication of the complexity of these structures and are found throughout the data comprising the geopolymerisation of potash, uranium, and base metal tailings. It is therefore still not clear whether these ions are bonded into the structure or whether the surrounding matrix is just physically encapsulating them.

If the contribution that the Pb ion makes to a stronger structure is of a physical nature, such as through more efficient packing or its larger radius, then one would expect the matrix to have less porosity compared to the weaker Cu-containing matrices. Since this is not the case, it is reasonable to assume that some kind of chemical bonding does take place and that the chemical nature of the immobilised ion also contributes to the formation of specific phases during synthesis. This statement will be substantiated more thoroughly in the next sections. It should be kept in mind that there would be a limit to the amount of contaminant any matrix can tolerate without losing all its structural integrity. At this point the presence of additional metal ions would serve to weaken the structure, although this limit is expected to be unique for every element and a function of both the chemical and physical properties of a specific ion.

Table 9
Influence of contaminant type and amount on the BET surface areas for the same matrix composition (m^2/g)

Matrix	Contaminant	Mass% of contaminant	Specific surface area
J1	Pb	1.0	1.9
J2	Pb	5.0	5.6
J3	Pb	10.0	5.7
J4	As	1.0	3.8
J5	As	5.0	4.5
J6	Cd	1.0	2.6
J7	Cd	5.0	9.8

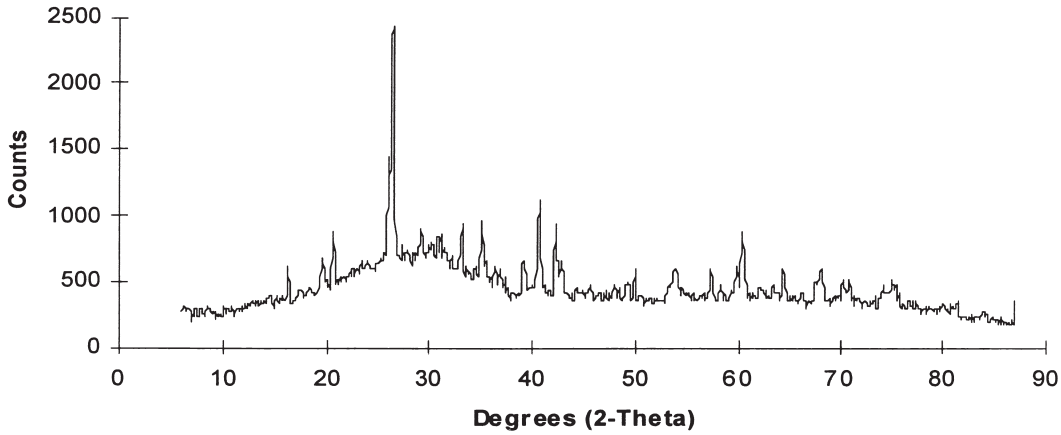

Fig. 1. XRD spectrum of matrix E1.

4.3. Specific surface area

It was mentioned earlier that structural effects caused by the addition of different metal contaminants are also reflected in the measured specific surface areas of geopolymerised fly ash. It seems that at lower concentrations of the contaminant (ca. 0.1% mass), slight changes to the structure could be affected slightly by the ionic radius of the metal, since these ionic sizes are of the same order of magnitude as the distances between neighbouring atoms in most of the crystalline and amorphous phases. From Table 7 it is evident that in each case the matrix that contains small amounts of Pb and has a slightly higher surface area than its Cu-containing counterpart. It therefore seems that the larger ionic size of the Pb atom does influence the polymer structure, thereby creating more surface area. As will be discussed later, this change could also be caused through chemical means since the phases present in the Cu- and Pb-containing matrices differ quite substantially. The incorporation of heavy metal contaminants into a commercially available geopolymer has also been reported [7] as resulting in a structure with increased porosity when compared to the pure geopolymer.

With reference to Table 9, an increase in the concentration of metal also leads to an increase in surface area when all other factors remain constant. At these very high concentrations, however, the rheology of the paste is affected by the added metal to such an extent that it can be visually observed as having different properties in the plastic state. This is especially true for Cd and would explain the large difference in specific surface area at concentrations of 1 and 5%, respectively. In the case of As, however, there also seems to be an increase in surface area, although As, unlike Cd and Pb, is very soluble at the conditions of synthesis that result in excess As not being physically or chemically encapsulated. Leaching data collected for previous studies [3] also substantiates this.

4.4. X-ray diffraction

It was previously observed [1–3] that the study of geopolymers using X-ray diffraction (XRD) is made difficult by the fact that a large part of the structure is amorphous to X-rays. A comparison of Figs. 1 and 2 and 3 shows a relatively large amorphous content between 20 and 40 degrees 2θ. This is much more pronounced in the case of E1

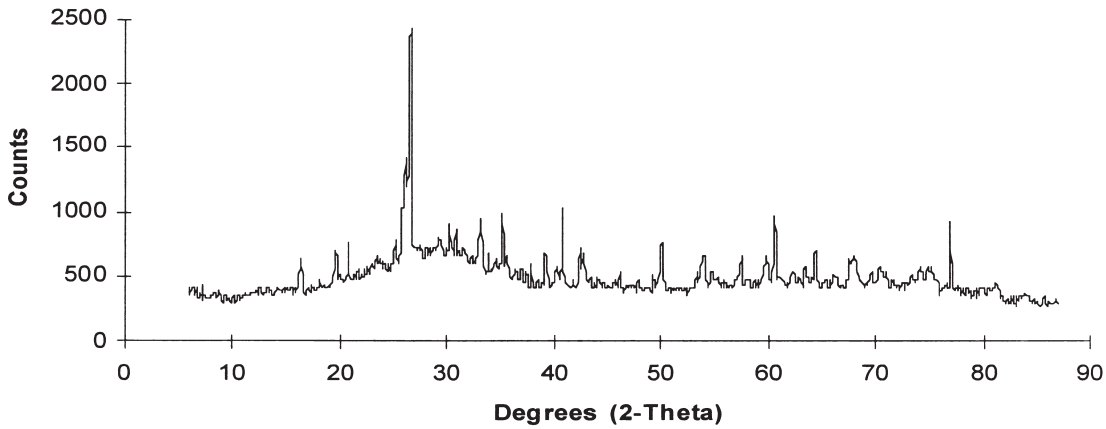

Fig. 2. XRD spectrum of matrix E2.

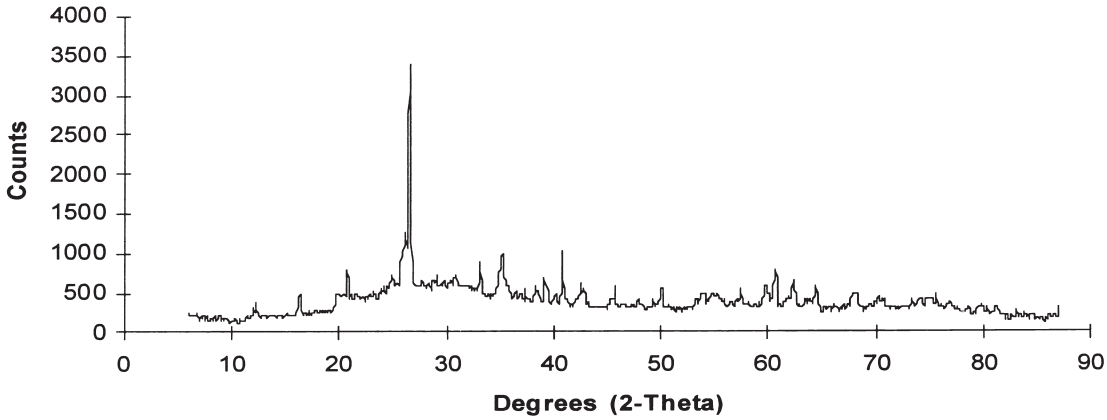

Fig. 3. XRD spectrum of matrix G1.

Table 10
Qualitative electron diffraction results for F1

Structure	d-spacing	Composition
Amorphous	3.5/2.2/1.2/1.1/0.8/0.7	Al, Si, Cu
Polycrystalline	1.3	Al, Si, Na, K, Ca, Fe, Cu
Polycrystalline	4.4/3.9/2.6/1.7/1.6/1.5/0.8	Al, Si, Na, K, Ca, Fe, Cu
Amorphous	Not available	Al, Si, K, Ca, Ti, Fe, Cu
Crystalline	Not available	Al, Si, Na, K, Ca, Fe

and E2 than that of G1, mainly because of an increased amorphous contribution by unreacted metakaolinite that is used in the synthesis of E1 and E2. The degree of crystallinity present is caused by quartz and mullite phases present in the fly ash. It can be seen, however, that a certain amorphous content is present in all of the samples, and this was further investigated by electron diffraction. As far as E1 and E2 are concerned, the different heavy metals included in each structure did not seem to make any difference to the crystalline part of the spectra and it is therefore assumed that the heavy metal bonds itself into the amorphous part of the matrix. This was also observed for matrices G1 (Fig. 3) and G2, and F1 and F2 (not shown). Further proof of this is supplied by electron diffraction studies, discussed below. XRD experiments conducted by a previous study [7] also failed to identify any substantial new phases that form in the crystalline part of the spectra.

Table 11
Qualitative electron diffraction results for F2

Structure	d-spacing	Composition
Amorphous	2.7/2.0/1.1	Al, Si, Na, K, Ca
Polycrystalline	3.1/2.7/2.1/1.2/0.7 3.4/2.2/2.0/1.7/1.3/1.2/	Al, Si, Ca
Polycrystalline	1.1/0.8/0.7/0.6	Al, Si, Ca
Amorphous	2.7/2.1/1.2/0.8/0.7/0.6	Al, Si, Na, K, Ca

4.5. Electron microscopy

Results from electron diffraction experiments are summarised in Tables 10 to 13 for F1, F2, E1, and E2 respectively. The electron diffraction study was conducted by concentrating on newly formed phases when comparisons with the starting materials were made. Therefore most diffractograms were recorded, which avoided obvious unreacted fly ash, kaolinite, and metakaolinite particles. In each case the calculated d-spacings were compared to that of metakaolinite, kaolinite, carbon, and fly ash, all of whose d-spacings are well documented in the literature, in order to ensure that they resemble a new phase. Each phase presented in Tables 10 to 13 therefore constitutes a newly formed structure. For every phase an elemental analysis was performed in order to further characterise its constituency. The detector used unfortunately could not analyse for Pb, although X-ray diffraction experiments suggested that the Pb is also taken up into the amorphous part of the structure.

With reference to Tables 10 and 11, it is of interest to note the fairly large differences in terms of d-spacings that occurred when the phases constituting F1 and F2 are compared. It is also apparent that most of the newly formed phases are either amorphous or polycrystalline. From Table 10 it is also evident that the Cu ions seem to be part of a the aluminosilicate structure in each case, since no copper oxides were found in the analyses. In most cases the inclusion of Cu also seems to be associated with the presence of Fe and this aspect needs to be investigated further. The relatively large difference in morphology as well as chemical composition between the various phases of F1 and F2 suggests that the metal contaminant does indeed influence the

Table 12
Qualitative electron diffraction results for E1

Structure	d-spacing	Composition
Amorphous	3.2/2.2/1.7/1.5/1.3	Al, Si, Na, K, Ca, Cu, Ti
Amorphous	3.2/2.2/1.7/1.3/0.8/0.7	Al, Si, K, Na, Ca, Cu
Amorphous	3.2/2.3/1.8/1.6/1.2/0.9/0.8/0.7	Al, Si, K, Ca, Cu

Table 13
Qualitative electron diffraction results for E2

Structure	d-spacing	Composition
Amorphous	2.1/1.5/1.3	Al, Si, Na, K, Ca, Fe
Amorphous	2.7/2.1/1.2/0.7	Al, Si, K, Na, Ca, Fe, S
Microcrystalline	3.1/2.7/2.1/1.6/1.3/1.2/ 1.0/0.8/0.7/0.6	A1, Si, K, Ca

chemistry of synthesis and therefore the physical and chemical properties of the final product.

The same is true when the different phases of E1 (Table 12) and E2 (Table 13) are compared. The Cu again seems to be part of the amorphous structure with most phases in E1 seemingly very closely related as far as both structure and chemical analyses are concerned. In the case of E2 the three phases seems structurally very different from one another, again suggesting that the presence of Pb both physically and chemically influences structure formation. The presence of Ca in most of the structures associated with the heavy metal is in accordance with an immobilisation model as proposed by Trezek et al. [12].

4.6. Infrared

Data from infrared (IR) experiments for matrices E1, E2, F1, F2, G1, and G2 are presented in Figs. 4 to 9 and the main feature of all IR spectra is the central peak between 1010 and 1040 cm^{-1} that is attributed to the Si-O-Si or Al-O-Si asymmetric stretching mode [13]. In comparing F1 and F2, it is obvious that the heavy metal does not seem to affect this peak, although there is a slight effect in the case of G1 (Fig. 8) and G2 (Fig. 9) with a shift of around 2 cm^{-1} when Pb is present instead of Cu. In the case of E1 (Fig. 4) and E2 (Fig. 5), however, this peak is found at 1025 and 1012 cm^{-1}, respectively, which indicates that the heavy metal does affect the structure and suggests that it might be part of the structure and not just physically encapsulated. The peak found at 543 cm^{-1} in Figs. 6 to 9 has previously been assigned to the bending of Si-O-Al, where the Al is in octahedral coordination [8]. It seems that the Pb ion only slightly influences this peak in the case of F2 (Fig. 7) and G2 (Fig. 9), compared to the Cu-containing matrices. E1 and E2 exhibit a peak each at 559 cm^{-1} that has been assigned to be originating from double-ring structures formed by Si and Al tetrahedra [13]. The fact that the added metal does not seem

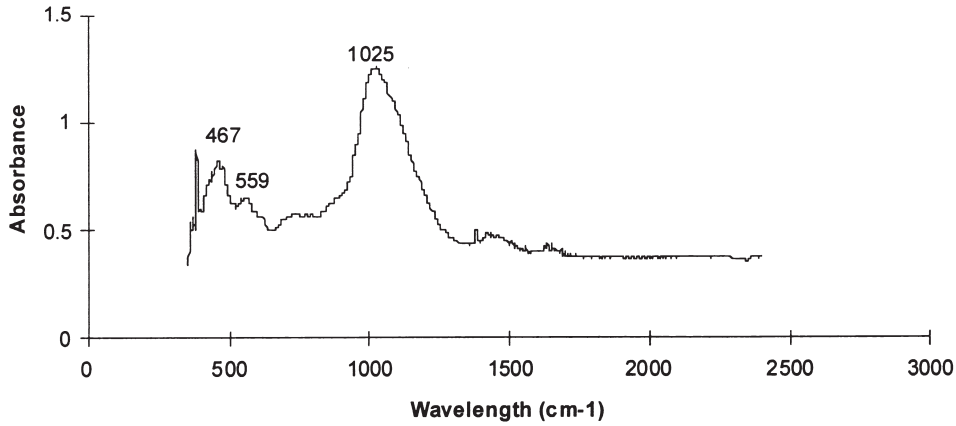

Fig. 4. IR spectrum of matrix E1.

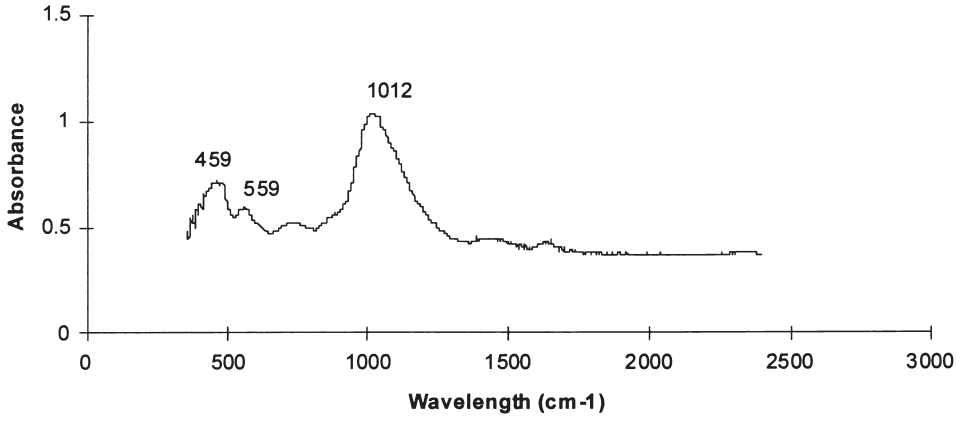

Fig. 5. IR spectrum of matrix E2.

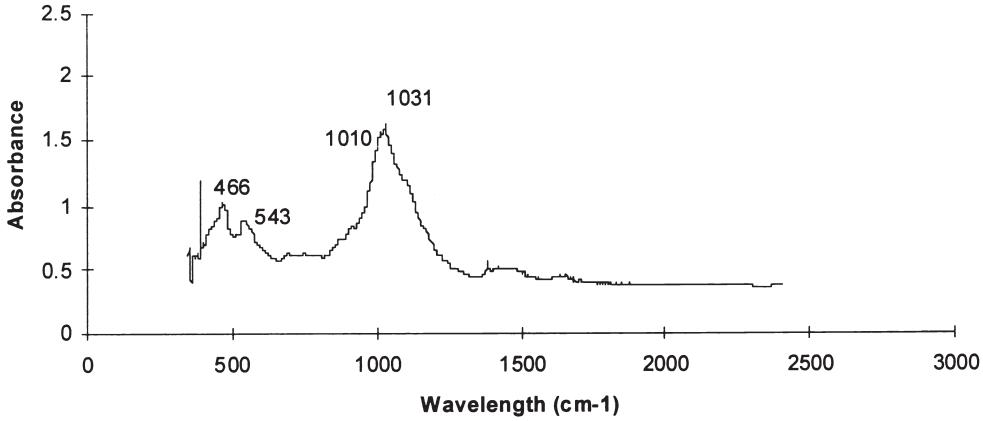

Fig. 6. IR spectrum of matrix F1.

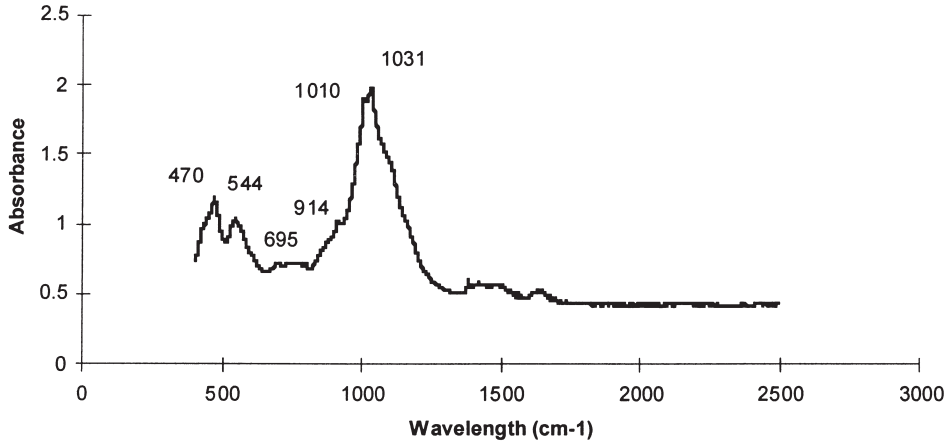

Fig. 7. IR spectrum of matrix F2.

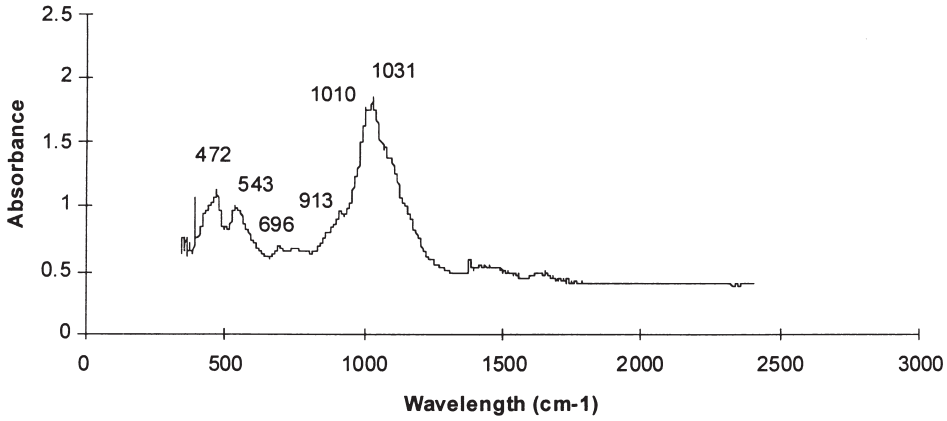

Fig. 8. IR spectrum of matrix G1.

to affect this ring formation also suggests that only certain parts of the polymer structure will be able to accommodate the inclusion and bonding of heavy metals. Perhaps the most significant peak shifts occur in the bands located between 450 and 480 cm^{-1}, which have been previously assigned to in-plane bending of the Si-O bonds found inside the basic aluminosilicate tetrahedron [14]. This shift can be found for all the matrices under consideration and indicates that the heavy metal does influence the environment of this bond to such an extent that different amounts of energy are

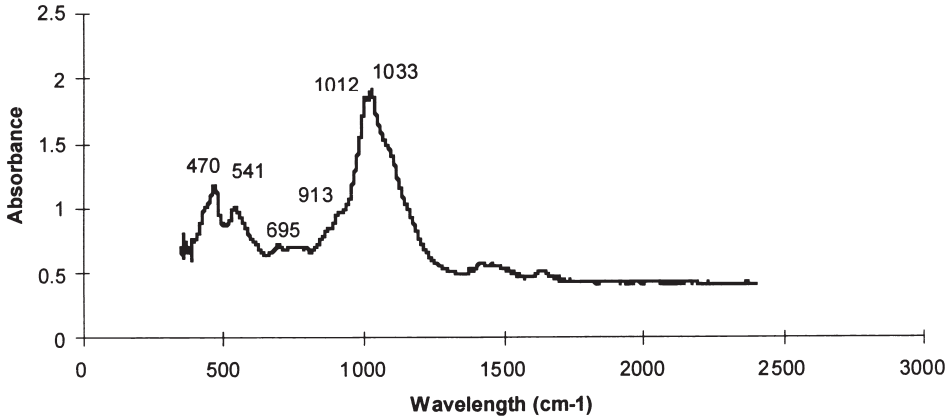

Fig. 9. IR spectrum of matrix G2.

required for the bending to take place. This effect is also influenced by the type of alkali metal used as activator [5], although that falls outside the scope of the present discussion.

4.7. NMR

Figs. 10 to 13 represent the ^{29}Si and the ^{27}Al MAS NMR spectra for matrices F1 and F2. In each case the ^{29}Si and ^{27}Al spectra of these matrices are identical, as one would expect if no substitution of Al and Si by the heavy metal occurs. The latter is highly unlikely for this kind of structure [15,16]. The ^{27}Al spectra of both F1 and F2 exhibit the same peak shifts of 58.5 and 2.2 ppm, which indicates a mixture of four and six coordinated Al [16,17]. In the case of the ^{29}Si spectra of F1 and F2, the two main shifts are −87.3 and −91.9 ppm, indicating an abundance of Si(4Al) and Si(3Al) sites [16,18], which is in accordance with other published structural information on geopolymers [19].

Since it is obvious that the added heavy metal does not change the basic tetrahedral building blocks of these aluminosilicate structures but does affect certain IR bending and stretching modes, one can conclude that incorporation of the

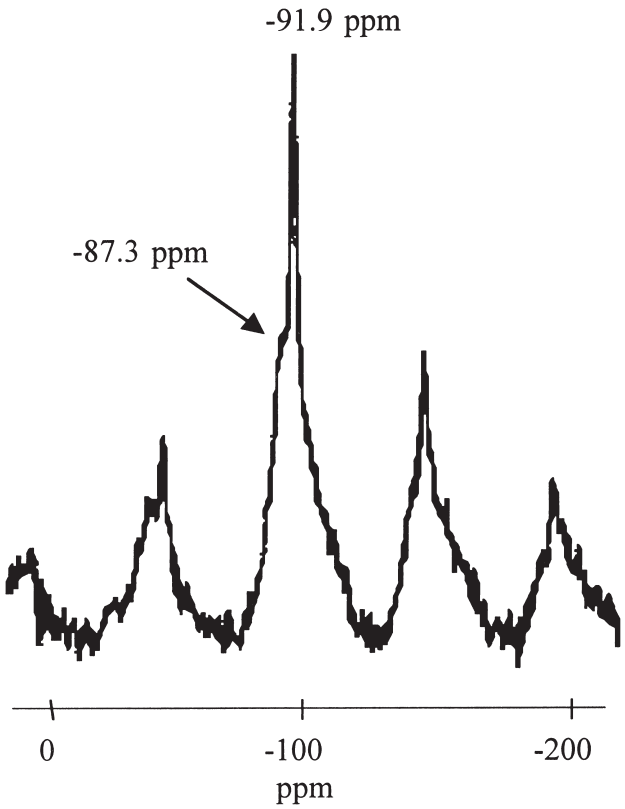

Fig. 10. ^{29}Si MAS NMR spectrum of F1.

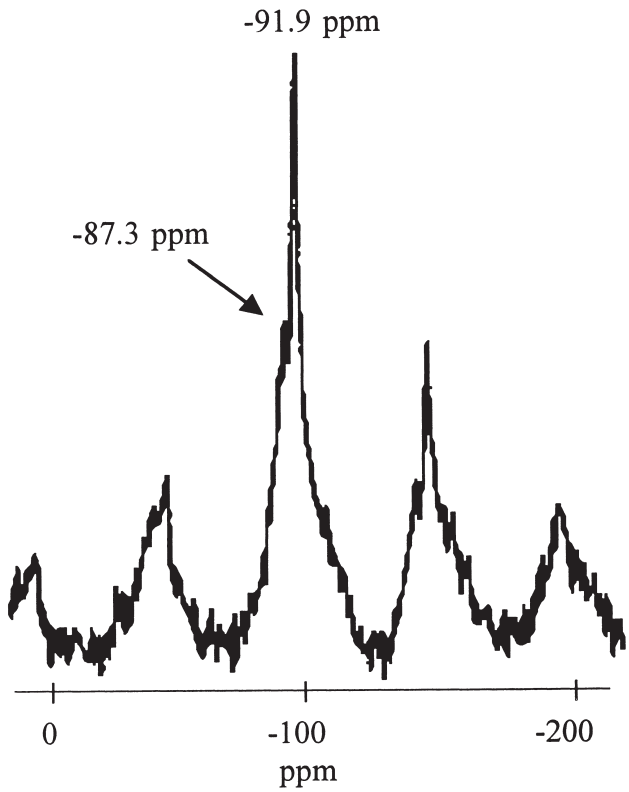

Fig. 11. ^{29}Si MAS NMR spectrum of F2.

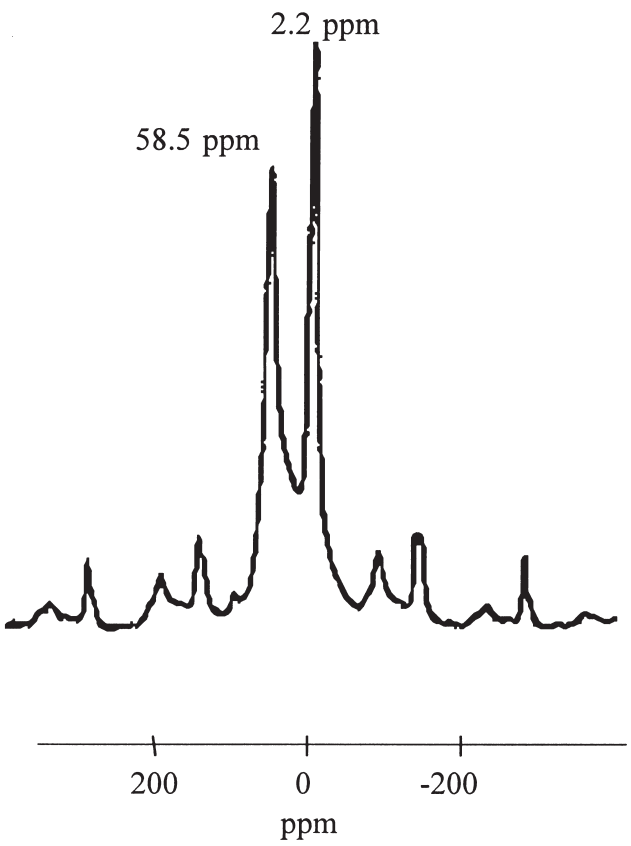

Fig. 12. ^{27}Al MAS NMR spectrum of F1.

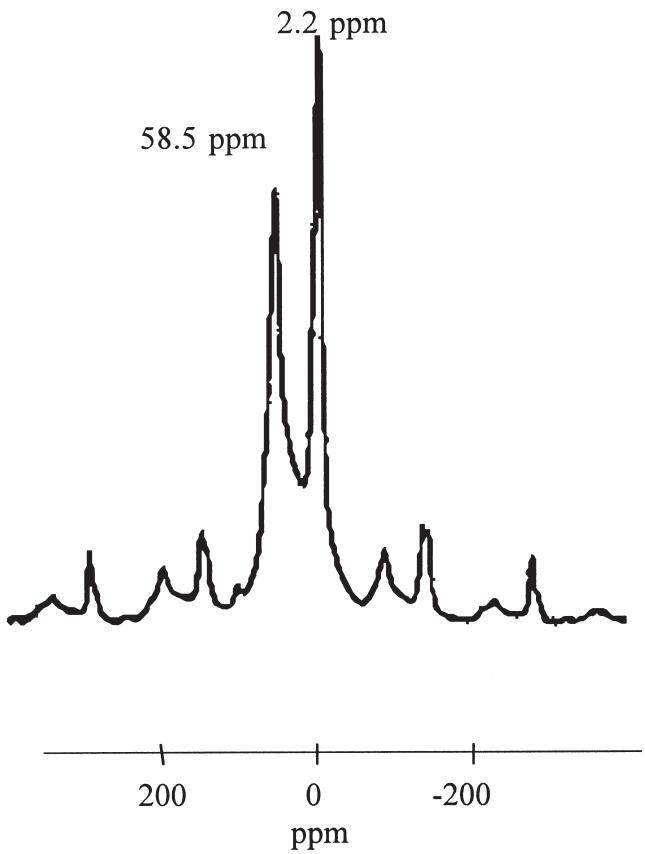

Fig. 13. ^{27}Al MAS NMR spectrum of F2.

metal contaminant takes place either through physical means, a charge-balancing action, or through covalent bonds, where the metal is bonded to the silicate chain through oxide and/or hydroxide links. The last option requires the presence of Ca [12] and other alkali and alkali earth ions that would also explain the presence of Ca in most of the new phases presented in Tables 10 to 13. It should be kept in mind, however, that the MAS NMR investigation presented here is very simplistic and a more thorough investigation centred around the metal itself will be necessary to fully quantify all the structural effects that result from the presence of the metal contaminants.

4.8. Leaching

Leaching studies are a very powerful tool to determine the immobilisation efficiencies of different ions in geopolymer systems. In a previous study [5] the potential of geopolymer binders for the immobilisation of heavy metals was discussed and environmental leaching results presented. It was also noted that different metal ions are immobilised with different efficiencies, a fact substantiated by data from other studies [3,4,6,7].

With reference to Table 14, the equilibrium values for both Cu and Pb are very similar as far as matrices E1 and E2 are concerned, although it was stated earlier that the latter matrix has a larger specific surface area than its Cu-containing counterpart. It could therefore be argued that the Pb ion should find it easier to leach out of the structure unless its relatively larger size offsets the effect of the increased surface area, which would result in a comparable equilibrium to that of Cu. Matrix breakdown was observed as being relatively little, but similar, in both cases. In comparison to the rest of matrices F1, F2, G1, and G2 in Table 14, it seems that Pb generally leaches less than Cu under the same conditions. It is also apparent that matrix G immobilises both Cu and Pb more efficiently than matrices E and F. The only difference between matrices G and F is the type of alkali metal used as activator, whereas the difference between matrices G and E is the thermal pretreatment of the kaolin used. These differences combined with the action of the metal contaminant during synthesis result in a wide variety of

Table 14
Equilibrium concentrations achieved during leaching with acetic acid for 24 h (ppm)

Matrix	Contaminant	212/600 μm	1700/2360 μm
E1	Cu	22	17
E2	Pb	23	17
F1	Cu	17	11
F2	Pb	11	8
G1	Cu	12	9
G2	Pb	<7	<7

Table 15
Equilibrium concentrations achieved during leaching with hydrochloric acid in stirred configuration for 24 h (ppm)

Matrix	Contaminant	600/1000 μm	2360/2800 μm
E1	Cu	18	8
E2	Pb	5	3
F1	Cu	22	27
F2	Pb	14	6
G1	Cu	32	17
G2	Pb	26	10

Table 17
Comparative percentages of metals leached from identical matrices under identical conditions with acetic acid in stirred configuration for 24 h (percent leached)

	Radius		
Geopolymer matrix	Fe (0.64/0.74)	Pb (0.84/1.20)	Hg (1.10/1.27)
Kaolin/sand	0.81	1.04	1.78
Kaolin/fly ash I	0.00	0.00	0.88
Kaolin/fly ash II	0.07	0.18	1.40

phases that cause structures with different chemical and physical characteristics, as explained earlier. The relative size of the cation does, however, play a role when diffusion occurs during leaching and cannot be discounted when predictions regarding long-term stability have to be made. Table 15 illustrates that these relative immobilisation efficiencies are independent of the leaching medium used, although different mineral phases seem to be attacked by the hydrochloric acid, which results in relatively better immobilisation efficiencies for matrix E than for matrix G.

As mentioned earlier, there seems to be a limit to the amount of heavy metal any matrix can tolerate. This point is illustrated by comparing the differences in leaching of Cu and Pb from matrices H1, H2, H3, and H4 (Table 16). Although H1 and H2 were synthesised with KOH and H3 and H4 were synthesised with NaOH, the latter group also contains double the amount of heavy metal that was introduced into the first. At smaller particle sizes H3 releases less Pb than the Cu released by H4, although this trend is reversed when the larger particle-size fractions are considered. This trend is not present in the case of H1 and H2 where the Cu always leaches more than the Pb. Referring to Table 7, the specific surface area of Cu-containing matrices H1 and H4 is smaller than that of their Pb-containing counterparts, although the latter seem to generally have a higher immobilisation efficiency.

Trezek et al. [12] suggested that in some cases the immobilisation of metals occurs through the formation of metal silicate chelates that serve to stabilise the polymeric silicate chains through active metal oxide and hydroxide bonds. These bonds are initially of a weak ionic character before being transformed into covalent bonds containing hydroxide, heavy metal, and alkali or alkali earth species. Although the purpose of this discussion is not to prove or disprove this representation, the resulting structure would be greatly influenced by the valence and ionic size of the included metal and alkali metal ions as these would find themselves in between the various polymeric chains that make up the structure. Leaching from these structures will therefore be influenced by the metal's ionic size in a major way. This can be substantiated to a certain extent by data obtained from the CANMET report for the leaching of stabilised base metal tailings, shown in Table 5. Results forming part of the present discussion and summarised in Table 17 fully support the above statement for three different geopolymer matrices. A study that focused on the immobilisation of radioactive substances in geopolymeric binders also concluded that for Sr, Cs, Mo, Tc, and U, the immobilisation efficiency depended largely on the valence and/or the ionic radius of the included metal cation. This covalent bonding of metal ions in between polymer chains would also be in accordance with NMR data presented earlier since no interference with the basic polymeric chain occurs.

Table 16
Equilibrium concentrations achieved during leaching with acetic acid in stirred configuration for 24 h (ppm)

Matrix	Contaminant	212/600 μm	1700/2360 μm	2360/2800 μm
H1	Cu	26.1	19.2	18.5
H2	Pb	9.1	8.4	8.2
H3	Pb	14.8	9.8	9.2
H4	Cu	17.1	7.5	6.3

5. Conclusions

The immobilisation of metal contaminants in various geopolymer structures does not only proceed by a physical encapsulation mechanism. It is concluded that different metal ions affect both the chemistry and morphology of structure formation during geopolymer synthesis, which results in various, mostly amorphous, phases being formed. It appears that the metal is chemically bonded to the structure, although the bonding does not affect the basic Al and Si tetrahedral building blocks that make up the bulk of the geopolymer phases. It does, however, affect the phase formation to such an extent that for the same quantities of identical starting materials, the final phases not only exhibits different physical characteristics but also slightly different chemical compositions and d-spacing values. Most of these effects on structure seem to be related to the ionic size and valence of a specific metal with larger ions having a tendency to be better immobilised and also more difficult to leach out. In certain instances increased concentrations of heavy metal contaminants can lead to a stronger structure. There would appear to be a limit as to the amount of metal a matrix can tolerate. However, this is also a function of other variables that were not discussed here, such as the alkali metal activator used, thermal history, and type of the starting materials, as well as the Si/Al ratio present in the final product. It was significant that the present study, which utilised waste materi-

als such as geopolymer reagents, provided for quite similar experimental results compared to previous studies conducted with more expensive commercial geopolymer binders.

References

[1] J.G.S. Van Jaarsveld, J.S.J. Van Deventer, L. Lorenzen, The potential use of geopolymeric materials to immobilise toxic metals: Part I. Theory and applications, Minerals Engineering 10 (7) (1997) 659–669.

[2] J.G.S. Van Jaarsveld, J.S.J. Van Deventer, L. Lorenzen, Factors affecting the immobilisation of metals in geopolymerised fly ash, Metallurgical and Materials Transactions B 29 (1998) 283–291.

[3] J. Davidovits, D.C. Comrie, J.H. Paterson, D.J. Ritcey, Geopolymeric concretes for environmental protection, Concrete International 12 (July 1990) 30–40.

[4] D.C. Comrie, New hope for toxic waste, The World and I (August 1988) 171–177.

[5] J.G.S. Van Jaarsveld, J.S.J. Van Deventer, A. Schwartzman, The potential use of geopolymeric materials to immobilise toxic metals: Part II. Material and leaching characteristics Minerals Engineering 21 (1998) 75–91.

[6] CANMET, Canada, DSS Contract No. 23440-6-9195/01SQ, Preliminary examination of the potential use of geopolymers for use in mine tailings management, Final Report, 1988.

[7] M.Y. Khalil, E. Merz, Immobilization of intermediate-level wastes in geopolymers, J Nuclear Materials 211 (2) (1994) 141–148.

[8] A. Madani, A. Aznar, J. Sanz, J.M. Serratosa, ^{29}Si and ^{27}Al NMR study of zeolite formation from alkali-leached kaolinites. Influence of thermal preactivation, J Physical Chemistry 94 (1990) 760–765.

[9] Australian Standard, AS 1012.9, Methods for testing concrete, 1986.

[10] US Government, Toxicity characteristic leaching procedure (TCLP), Federal Register 55, 11798–11877, 1990.

[11] CRC Handbook of Chemistry and Physics, 55th ed., CRC Press, Cleveland, Ohio, 1974, pp. F198–F199.

[12] G.J. Trezek, G. Raphael, J.S. Wilbur, R.E. VanPelt, Remediation of arsenic contaminated soil using polysilicates, HMCRI R&D '92 Conference, San Francisco, February 1992.

[13] E.M. Flanigan, H. Khatami, H.A. Szymanski, Molecular sieve zeolites, in: E.M. Flanigan, L.B. Sand (Eds.), Advances in Chemistry Series 101, American Chemical Society, Washington, D.C., 1971, pp. 201–229.

[14] J.D. Ortego, Y. Barroeta, F.K. Cartledge, H. Akhter, Leaching effects on silicate polymerisation. An FTIR and ^{29}Si NMR study of lead and zinc in portland cement, Environmental Science and Technology 25 (1991) 1171–1174.

[15] R.M. Barrer, Hydrothermal Chemistry of Zeolites, Academic Press, New York, 1982.

[16] J. Klinowski, Nuclear magnetic resonance studies of zeolites, Progress in NMR Spectroscopy 16 (1984) 237–309.

[17] E. Lipmaa, A. Samoson, M. Magi, High-resolution ^{27}Al NMR of aluminosilicates, J American Chemical Society 108 (1986) 1730–1735.

[18] E. Lipmaa, A. Samoson, M. Magi, M. Tarmak, G. Engelhardt, Investigation of the structure of zeolites by solid-state high resolution ^{29}Si NMR spectroscopy, J American Chemical Society 103 (1981) 4992–4996.

[19] J. Davidovits, Geopolymers: Inorganic polymeric new materials, J Materials Education 16 (1994) 91–138.